MODELING CIRCUITS WITH OPERATIONAL TRANSCONDUCTANCE AMPLIFIERS USING WAVE DIGITAL FILTERS

Ólafur Bogason

CIRMMT
McGill University
Montreal, Canada
olafur.bogason@mail.mcgill.ca

Kurt James Werner

The Sonic Arts Research Centre (SARC)
School of Arts, English and Languages
Queen's University Belfast, UK
k.werner@qub.ac.uk

ABSTRACT

In this paper, we show how to expand the class of audio circuits that can be modeled using Wave Digital Filters (WDFs) to those involving operational transconductance amplifiers (OTAs). Two types of behavioral OTA models are presented and both are shown to be compatible with the WDF approach to circuit modeling. As a case study, an envelope filter guitar effect based around OTAs is modeled using WDFs. The modeling results are shown to be accurate when to compared to state of the art circuit simulation methods.

1. INTRODUCTION

A component commonly found in audio circuits is the operational transconductance amplifier (OTA) [1, 2, 3, 4]. Audio gear that contains it includes famous guitar effects pedals [5, 6], voltage controlled amplifiers and oscillators [7, 8, 9]. Despite its wide usage in audio circuits, little research on OTAs in the Virtual Analog context is available [10]. Understanding both idealized and non-idealized models of OTAs and how to apply them in common physical modeling frameworks, such as the state-space model [11, 12] or Wave Digital Filters (WDFs) [13], is paramount if circuits containing them are to be accurately modeled.

WDFs provide an elegant framework for creating digital models of analog reference circuits, or other lumped physical systems [14]. Until recently, the scope of circuits that were tractable using standard WDF techniques was limited to circuits composed of linear components, connected in series and/or parallel and could contain up to one nonlinearity. Although researchers have, in special cases, been able to go beyond these limitations by exploiting topologies of reference circuits [15, 16, 17, 18, 19] or by adding fictitious unit delays to yield computable structures [20, 21], the aforementioned limitations made simulating most audio circuits unfeasible within the WDF framework.

By incorporating Modified Nodal Analysis from Circuit Theory [22], along with grouping nonlinearities into a vector at the root of a WDF tree [16, 23], recent research has provided new theoretical ground which facilitates the modeling of most audio circuits using WDFs. This approach requires that each component in the reference circuit has a suitable Kirchhoff domain model. In this paper we will leverage the recent theoretical advancement to provide two models for the OTA which are suitable for use in WDFs.

This paper is structured as follows: §2 reviews OTAs and presents an ideal model and non-ideal linear macromodel in the Kirchoff domain. §3 discusses recent theoretical advancements in WDF theory and how they have permitted us to derive wave-domain OTA models from Kirchoff-domain models. It furthermore outlines how to incorporate the newly derived models to simulate circuits containing OTAs using WDFs. §4 builds upon the derived OTA models and derives WDFs of an envelope filter reference circuit. §§5–6 discusses the accuracy of the proposed model, discusses future work and concludes.

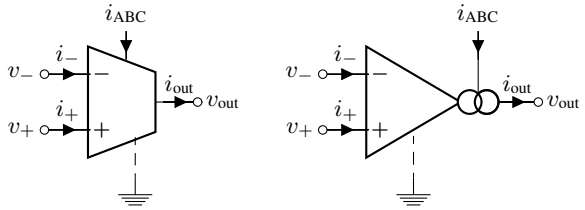

(a) *VCCS-Based OTA Symbol.* (b) *Alternate OTA Symbol.*

Figure 1: *OTA symbols*

2. OPERATIONAL TRANSCONDUCTANCE AMPLIFIERS

OTAs are active, tunable, high-gain devices, that take differential voltage as input and output current. The external tuning of the gain, termed *transconductance*, make OTAs the perfect building block for audio circuit designers. By modifying the transconductance, OTAs are most commonly used to decouple control from audio circuitry, as is done in the filter of the MS-20 synthesizer [9] or in the envelope filter discussed in §4.

OTAs may be built using bipolar or CMOS transistor technology [4]. CMOS OTAs are widespread in high-frequency applications [24] but are less common in audio circuits where bipolar OTAs are ubiquitous.

On the device level modern OTAs can be quite complex, containing multiple transistors and other nonlinear components in complicated topologies. To simplify circuit design, analysis, and simulation, OTA behavior is often idealized completely or approximated, as is often done with traditional op amps [25]. Such approximations include linear [26] or nonlinear macromodels [27].

The OTA symbol most commonly used by the research community is the VCCS symbol augmented with an additional bias current port as shown in Figure 1a. The OTA symbol widely found in circuit schematics is shown in Figure 1b.

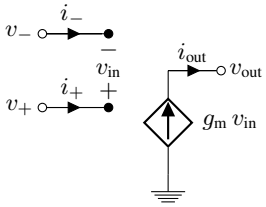

Figure 2: *Ideal OTA*

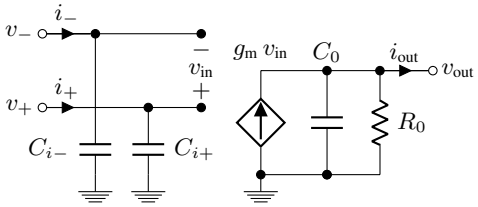

Figure 3: *Macromodel OTA*

2.1. Ideal VCCS Model of an OTA

An ideal OTA is a voltage dependent current source, with an adjustable gain, called transconductance g_{m} [4]. The output current i_{out} is equal to the multiplication of the differential voltage input $v_{\text{in}} = v_+ - v_-$ and g_{m}

$$i_{\text{out}} = g_m\, v_{\text{in}}\,. \tag{1}$$

The conductance between the input terminals is assumed zero as is the case with traditional op amps [25]. The output is assumed to be a current source and so the output impedance is large. This is not the case for the standard op amp which exhibits low impedance at its output terminal. Low output impedance is often desirable when designing audio circuits and so modern bipolar OTAs, such as the LM13700 [28], include controlled impedance buffers on device.

The transconductance of a real world device is a multivariate dynamic nonlinear function, dependent on temperature, device geometry, the manufacturing process, etc. [27, 29]. In the ideal case it is a simple function on temperature and a bias current, which the device sinks through a dedicated input terminal. This bias current is often referred to as the Amplifier Bias Current i_{ABC}. For an OTA based on a bipolar transistor differential pair, the output current and transconductance are given by [3, 4]

$$i_{\text{out}} = i_{\text{ABC}} \tanh \frac{v_{\text{in}}}{2\,V_{\text{T}}} \tag{2}$$

$$g_{\text{m}} = \frac{di_{\text{out}}}{dv_{\text{in}}} = \frac{i_{\text{ABC}}}{2\,V_{\text{T}}} \operatorname{sech}^2 \frac{v_{\text{in}}}{2\,V_{\text{T}}} \tag{3}$$

In this equation the transconductance depends instantaneously on the differential input voltage. It is however desirable for circuit designers if the transconductance is independent on the differential voltage input as discussed in §2. Assuming that $|v_{\text{in}}| \ll 2V_{\text{T}}$ the transconductance becomes

$$g_{\text{m}} \approx \frac{i_{\text{ABC}}}{2\,V_{\text{T}}} \tag{4}$$

V_{T}, the thermal voltage, is usually on the scale of tens of millivolts and so making this assumption limits the dynamic range of the input. However, modern OTAs, such as the LM13700 [28], include linearizing diodes that increase the input range of the differential voltage input while keeping the transconductance gain linear with respect to i_{ABC} [3].

Methods on how to handle nonlinearities in WDFs have been proposed in the past. Some have involved the introduction of ad-hoc unit delays [19, 18, 30], simplification of nonlinear devices [17, 31], or ad-hoc [21] or systematic [32] global iteration. A systematized method, sidestepping the aforementioned limitations, was proposed in [23]. To balance accuracy, physical interpretability and complexity we make the simplification that the transconductance is a linear function of i_{ABC}, as in (4).

Modified Nodal Analysis (MNA) is a systematic way to keep track of physical quantities within a circuit [33]. The method becomes automatable by *stamping* each component into a MNA matrix. MNA element stamps will also work with the Nodal DK-method for deriving nonlinear state-space systems [12] and in §3 we will describe how to transfer a populated MNA matrix from the Kirchoff domain to the wave domain [22]. An ideal OTA is shown in Figure 2 while a MNA element stamp is given by (5).

$$\begin{array}{c} \\ \gamma \\ \delta \\ \text{next} \end{array} \begin{array}{c} \begin{array}{ccc} \alpha & \beta & \text{n} \end{array} \\ \left[\begin{array}{ccc|c} & & & 1 \\ & & & -1 \\ \hline -g_{\text{m}} & g_{\text{m}} & & -1 \end{array}\right] \end{array} \tag{5}$$

Nodes shown in Figure 2 are $\alpha = v_+$, $\beta = v_-$, $\gamma = v_{\text{out}}$, $\delta =$ ground.

2.2. OTA Macromodel

Real-world OTAs exhibit multiple nonidealities. Some of which may lead to audible effects and need to be taken into account when designing or analyzing audio circuits. Similar to the nonidealities exhibited by standard opamps [25], real-world OTAs have finite input and output conductances and capacitances, input offset voltage, input bias currents, input offset current, differential and common mode gain and also other OTA-specific nonidealities such as frequency dependent transconductance gain [26].

Choosing which effects to include in a macromodel is a trade-off between complexity and accuracy. Complex nonlinear macromodels for CMOS OTAs exist in the literature [27] and can be adapted to bipolar OTAs by tuning the model parameters. In this paper we balance complexity and accuracy by proposing a linear macromodel which models input and output capacitances C_{i+}, C_{i-} and C_o as well as a finite output conductance R_o.

3. WAVE DIGITAL FILTERS

Here, we briefly elaborate on the recent theoretical developments that have allowed us to model circuits containing OTAs using WDFs techniques. For the sake of brevity a detailed discussion on WDF theory is omitted. The interested reader is referred to the classic article by Fettweis [13] and other recent work in the field [17, 34, 35, 36].

The scattering behavior of multiport series and parallel adaptors has been known since the 1970s [37]. The issue with complicated topologies that can not be divided into series and/or parallel adaptors was first recognized by Martens and Meerkötter [38].

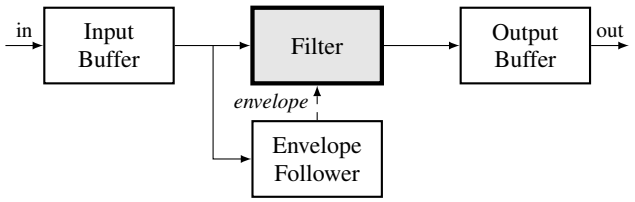

Figure 4: *An abstract building block diagram of an envelope filter.*

They used a graph-theoretic approach to find the scattering matrix of an adaptor with complicated topology, relying heavily on the orthogonality of the reference circuit for their derivation. Although their method was a step in the right direction, it could not be used to derive scattering matrices for circuits containing common audio circuit devices, such as op amps, OTAs, or controlled sources.

A derivation of the scattering matrix for arbitrary topologies was outlined by Werner *et al.* in [22]. Thévenin sources are placed at each port of a $\mathcal{R}$-type adaptor and a MNA matrix is populated. By treating all incident and reflected waves simultaneously by grouping them together as vectors $\boldsymbol{b}$ and $\boldsymbol{a}$, a scattering matrix $\mathbf{S}$ describing the relationship between the waves, $\boldsymbol{b} = \mathbf{S}\,\boldsymbol{a}$, is given by

$$\mathbf{S} = \mathbf{I} + 2\,\mathbf{R}\,[\mathbf{0} \quad \mathbf{I} \quad \mathbf{0}]\,\mathbf{X}^{-1}\,[\mathbf{0} \quad \mathbf{I} \quad \mathbf{0}]^{\intercal} \tag{6}$$

where $\mathbf{R}$ is a diagonal matrix containing the Thévenin/port resistances and $\mathbf{X}$ is the populated MNA matrix.

An important detail of this approach is that controlled sources may be absorbed into the scattering matrix itself. This is traditionally done with MNA matrices [33] but also in WDF theory by absorbing sources or resistors into adaptors [13]. Absorbing sources into a scattering matrix in this manner is what enables us to model arbitrary circuits containing OTAs.

3.1. OTAs in WDFs

The process of deriving a WDF model of a reference circuit that contains OTAs follows in a similar manner as in [25]. Starting with a reference circuit, replace existing OTAs with an ideal model or macromodel. Following the steps in [39], a WDF structure is found and for each $\mathcal{R}$-type adaptor, (6) is used to determine its scattering matrix.

The resulting WDF structure can be represented by a SPQR tree that is used to visually indicate how one computation cycle is carried out. For reference circuits that contain OTAs, one additional step must be taken at each cycle as transconductance parameters that reside within $\mathcal{R}$-type adaptors must be computed and the scattering matrix for each $\mathcal{R}$-type adaptor updated accordingly.

4. CASE STUDY

In this case study we use the derived OTA models to model an envelope filter guitar effect [1] using WDF techniques. An envelope filter works by tracking the temporal envelope of an input signal. The envelope is used to modulate the critical frequency of a filter, that in turn is used to filter the input. The general structure of the envelope filter can be divided into several abstract building blocks shown in Figure 4.

[1] Based on `http://topopiccione.atspace.com/PJ11DODfx25.html`

Table 1: *Component values*

Component	Value
R_{10}	$10\,\mathrm{k\Omega}$
$R_{11}, R_{12}, R_{17}, R_{18}$	$1\,\mathrm{k\Omega}$
$R_{13}, R_{15}, R_{16}, R_{19}, R_{20}$	$22\,\mathrm{k\Omega}$
R_{14}	$100\,\mathrm{k\Omega}$
C_6	$1\,\mu\mathrm{F}$
C_7, C_8	$10\,\mathrm{nF}$

The derivation of a WDF structure for the entire envelope filter will be presented in detail in an upcoming master thesis [40]. In this paper we will concentrate on the section of the guitar effect that contains OTAs, namely the filter circuit. The circuit schematics of the filter are shown in Figure 5 and the component values are listed in Table 1.

In order to simplify the schematics, we idealize each Darlington transistor pair as an ideal buffer via the circuit theoretic steps detailed in Figure 6. Assuming a transistor operates ideally, it can be replaced by a nullor (step 1) [41, 42]. The junction of two nullators and a norator is equivalent to a single norator (step 2). Finally, a norator in series with any normal one-port is equivalent to just a norator (step 3) [43]. What remains is an ideal (nullor) buffer for each Darlington pair.

This step implies that the voltage drop over the PN-junctions of the Darlington pair is 0 V. As we will see in §5 this assumption does not appear to have a great impact on the output signal. Furthermore, any dc bias that is introduced by this voltage drop would be filtered away in the output buffer stage.

The presence of the nullors also implies that certain electrical components can be dropped from the circuit without affecting its behavior. Specifically, R_{13} and R_{19} and their two series voltage sources v_{EE} end up in parallel with norators coming from the Darlington pairs, an arrangement which is equivalent on a circuit-theoretic level to just a norator [43]. Therefore R_{13} and R_{19} and their series voltage sources v_{EE} are removed from the circuit in preparation for forming the WDF model.

A final transformation to the circuit involves the input stage of the circuit (v_{in}, R_{10}, and C_6). In this stage, R_{10} and C_6 are swapped, as shown in Fig. 7a. This does not affect the dynamics of the circuit, but does ease the implementation as a WDF by allowing R_{10} to be associated directly with v_{in}, forming a resistive voltage source which is suitable for inclusion anywhere in a WDF structure. This transformation does however affect the polarity of the components. An additional inverter, $\mathcal{I}_1$, must be included in the structure to obtain correct polarization [36, 44].

4.1. Filter Description Assuming Ideal OTA

To gain insight into which kind of filter the circuit is realizing we derive its transfer function. We replace the OTA with our ideal model and assume that i_{ABC} and the range parameter are constants, i.e., we study the system under LTI conditions. We continue to derive the transfer function using MNA (and the newly derived OTA MNA element stamps) [45].

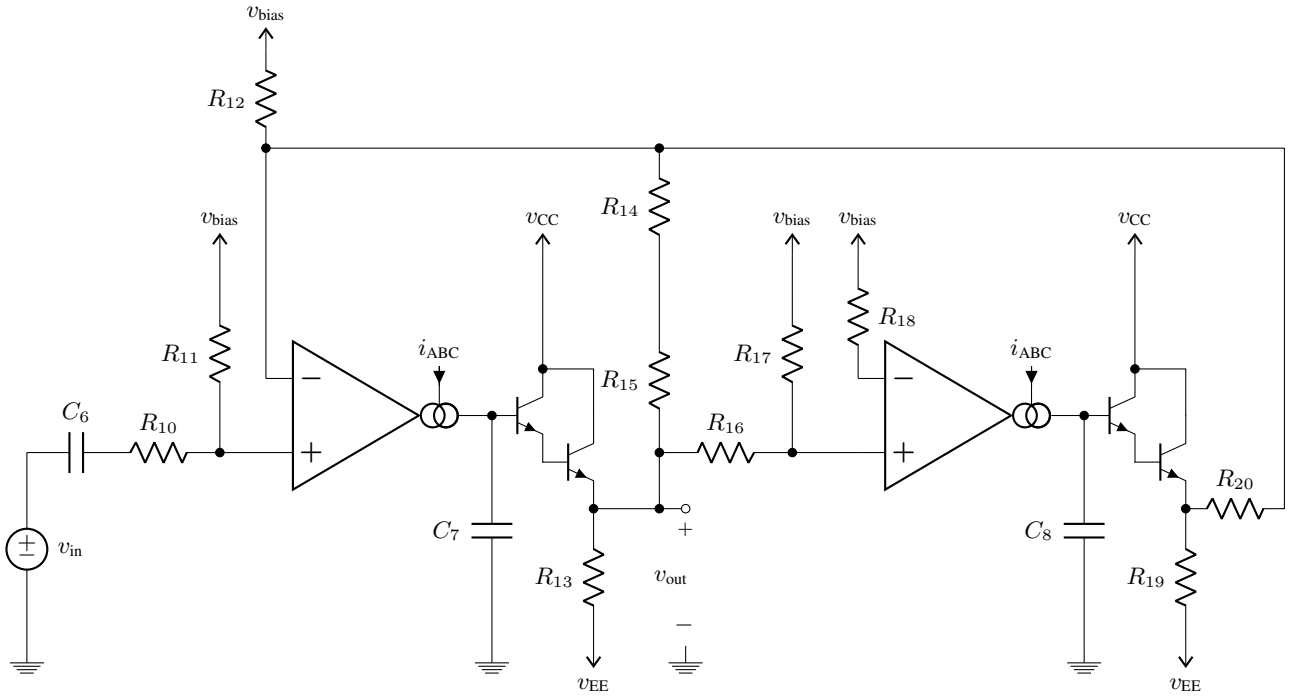

Figure 5: *Filter circuit schematic.*

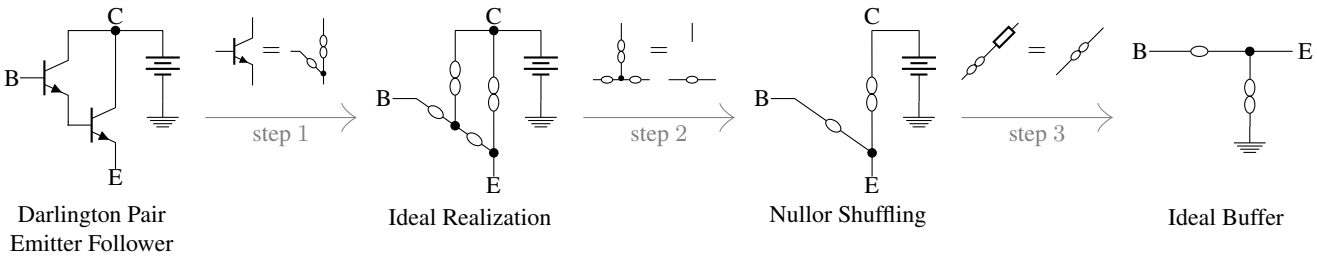

Figure 6: *Darlington pair emitter follower to idealized nullor realization.*

$$H(s) = \underbrace{H_0}_{\text{Gain}} \underbrace{\frac{s}{s+\omega_\text{c}}}_{\text{Highpass section}} \underbrace{\frac{\frac{\omega_0}{Q_\infty}s}{s^2+\frac{\omega_0}{Q_\infty}s+\omega_0^2}}_{\text{Bandpass filter}} \tag{7}$$

The transfer function this circuit realizes is essentially a 1st order highpass filter, composed of components C6, R10 and R11, cascaded with a 2nd order bandpass filter [46]. To simplify the expression of the transfer function components with identical values are grouped together, $R_\text{a} = R_{10}$, $R_\text{b} = R_{11}, R_{12}, R_{17}, R_{18}$, $R_\text{c} = R_{15}, R_{16}, R_{20}$, $R_\text{d} = R_{14}$, $C_\text{a} = C_6$ and $C_\text{b} = C_7, C_8$. We define $R_\text{q} = R_c + rR_d$, where $r \in]0, 1]$ determines the range.

$$\omega_\text{c} = \frac{1}{C_\text{a}\left(R_\text{a}+R_\text{b}\right)} \tag{8}$$

$$H_0 = \frac{\frac{R_\text{b}R_\text{c}}{R_\text{q}} + R_\text{b} + R_\text{c}}{3\left(R_\text{a}+R_\text{b}\right)} \tag{9}$$

$$\omega_0^2 = \frac{R_\text{b}^2\, g_\text{m}^2}{C_b^2\left(R_\text{b}+R_\text{c}\right)\left(\frac{R_\text{b}R_\text{c}}{R_\text{q}} + R_\text{b} + R_\text{c}\right)} \tag{10}$$

$$Q_\infty = \frac{R_\text{q}}{R_\text{c}}\sqrt{\frac{\frac{R_\text{b}\,R_\text{c}}{R_\text{q}} + R_\text{b} + R_\text{c}}{R_\text{b}+R_\text{c}}}\,. \tag{11}$$

Interestingly R_q, controlled by the range, influences all parameters of the transfer function except ω_c. The transconductance, g_m, whose highest value can be set by the sensitivity knob in the envelope follower section, only influences the center frequency. That means that the filter is a constant-Q filter with respect to the transconductance, surely a desirable trait when sweeping the frequency spectrum.

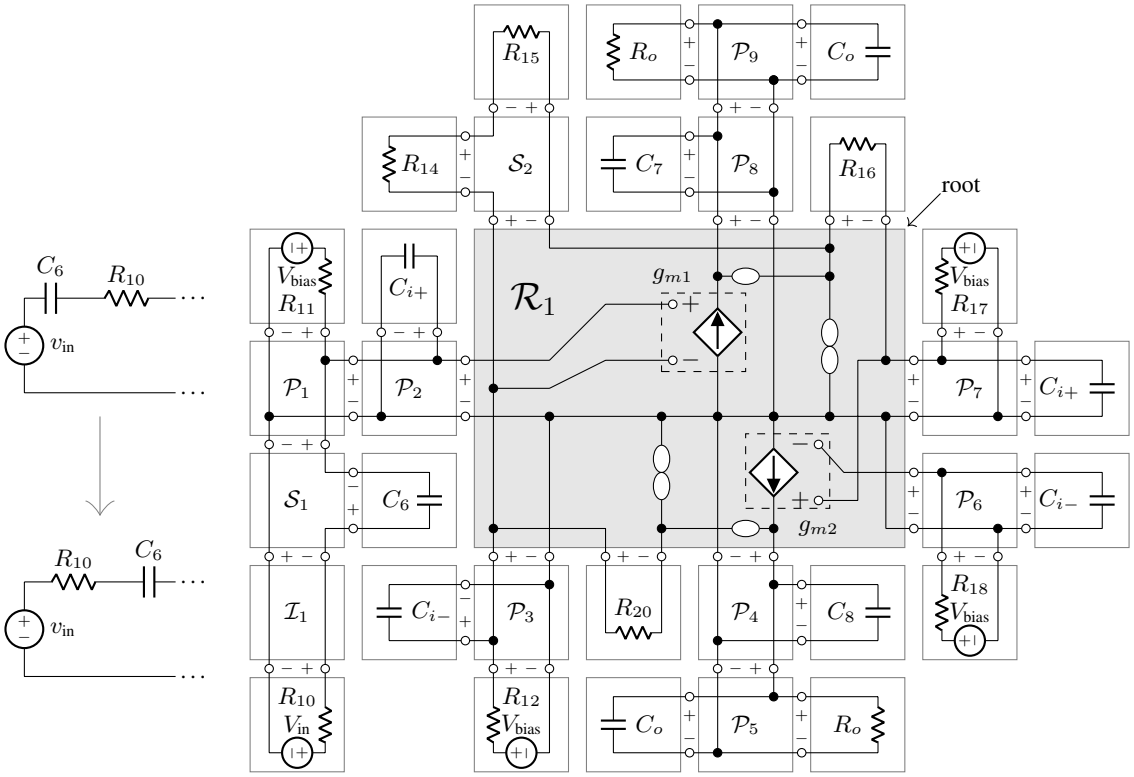

(a) Input stage equivalence.

(b) Rearranging circuit to highlight Wave Digital Filter structure.

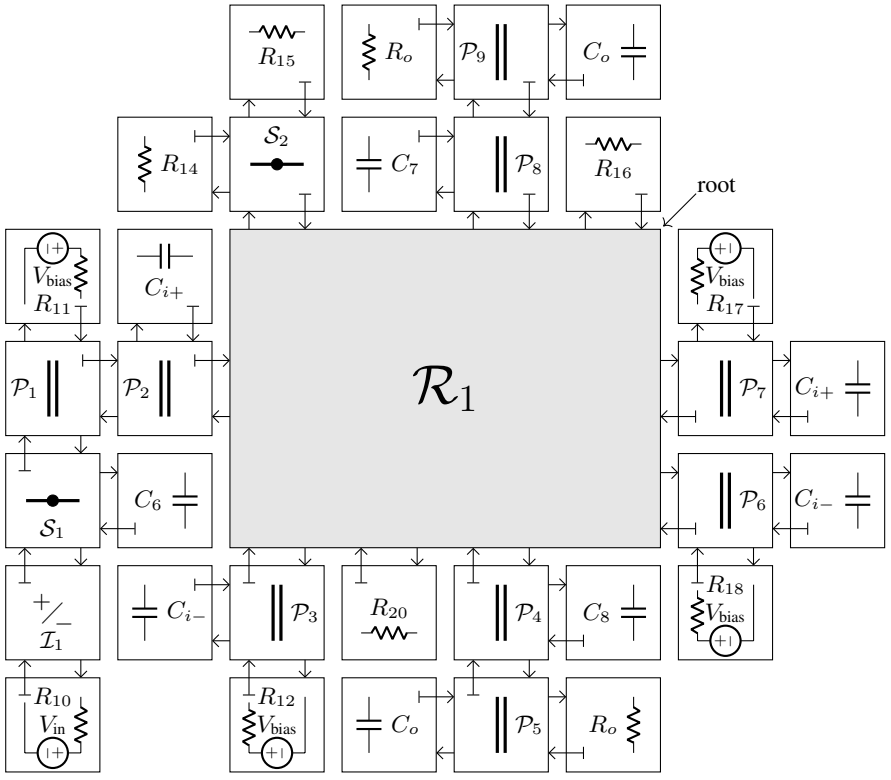

(c) Wave Digital Filter structure.

Figure 7: *Setting up circuit to highlight topology, and corresponding Wave Digital Filter structure.*

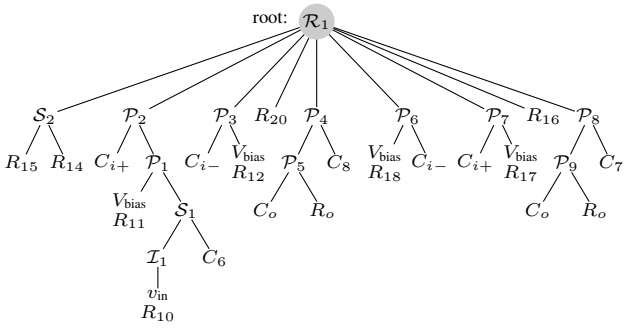

Figure 8: *Macromodel OTA—Filter SPQR tree*

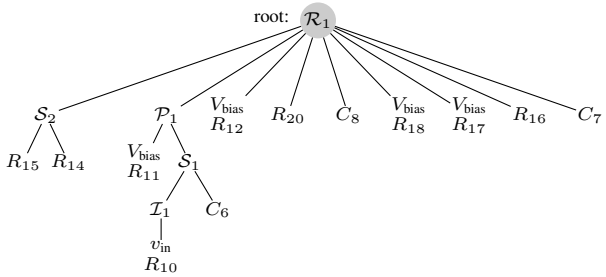

Figure 9: *Ideal OTA—Filter SPQR tree.*

4.2. WDF Using Macromodel OTA

By first modeling the filter using the macromodel OTA we can show how to derive the complete WDF structure. In §4.3 we simplify this WDF to model the ideal OTA case. We chose the macromodel parameters $C_{i+} = C_{i-} = 5\,\text{pF}$, $C_o = 700\,\text{pF}$ and $R_o = 50\,\text{M}\Omega$ so that a Bode plot of the macromodel-based filter matches a Bode plot of a component-level-based model [2].

We proceed to model the filter by following the steps described in §3.1. We limit the size of the resulting $\mathcal{R}$-type adaptor by absorbing resistors into the bias voltage sources V_{bias}. Capacitors are discretized using the bilinear transform. The filter circuit rearranged to highlight the WDF structure is shown in Figure 7b while the corresponding WDF structure is shown in Figure 7c.

4.3. WDF Using Ideal OTA

For the ideal OTA case we simply remove the components belonging to the macromodel (both R_o, both C_o, both C_{i-}, and both C_{i+}) and follow the same procedure as before. Again choosing the $\mathcal{R}_1$ adaptor as the root, the SPQR tree for the resulting WDF structure is given in Figure 9.

5. RESULTS

Comparison of Bode plots with three amplifier bias currents $i_{\text{ABC}} = \{6, 60, 600\}\,\mu\text{A}$ and four range settings $r = \{0.01, 0.22, 0.6, 1.0\}$ are shown in Figure 10. The input is supplied via the ideal voltage source, v_{in}, and output at taken at v_{out} in Figure 5.

The ideal OTA based circuit shows excellent results when compared to the transfer function. The only visible difference between

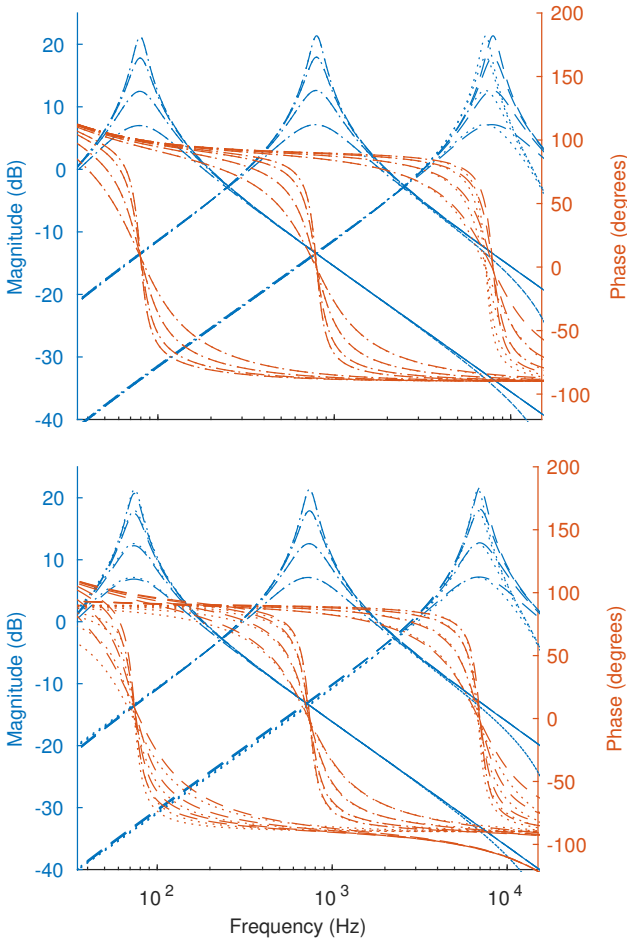

Figure 10: *Bode plot comparison of magnitude (blue) and phase (orange) spectrums. Upper plot compares the ideal OTA transfer function (dashed lines) and WDF model (dotted lines). Lower plot compares the component-level SPICE model of the LM13700 (dashed lines) with a macromodel-based model (dotted lines).*

to two happens as the frequency approaches the Nyquist frequency where the warping effects from the bilinear transform become noticeable. The plot of the macromodel is in good accordance with a component-level SPICE model where the magnitude spectrum matches almost exactly throughout the range of amplifier bias currents and range controls. There are minor differences in the location of critical frequencies and bandwidth between the two plots in Figure 10.

We briefly study the circuit's behavior under time-varying conditions. The input is a 440 Hz sawtooth, r, the parameter controlling the range, is set to 0.01 and i_{ABC} is increased linearly over time as indicated in the first row of Figure 11. In the second row of the same figure a comparison of a SPICE simulation of the filter circuit composed of an ideal OTA simulated using SPICE is compared to the ideal OTA WDF. The third row compares the ideal and macromodel WDFs to a component-level model of the LM13700 OTA as simulated in SPICE. Despite the assumptions of (4) and idealizing Darlington pairs as ideal buffers, good results are obtained.

[2] `http://www.idea2ic.com/LM13600/SpiceSubcircuit/LM13700_SpiceModel.html`

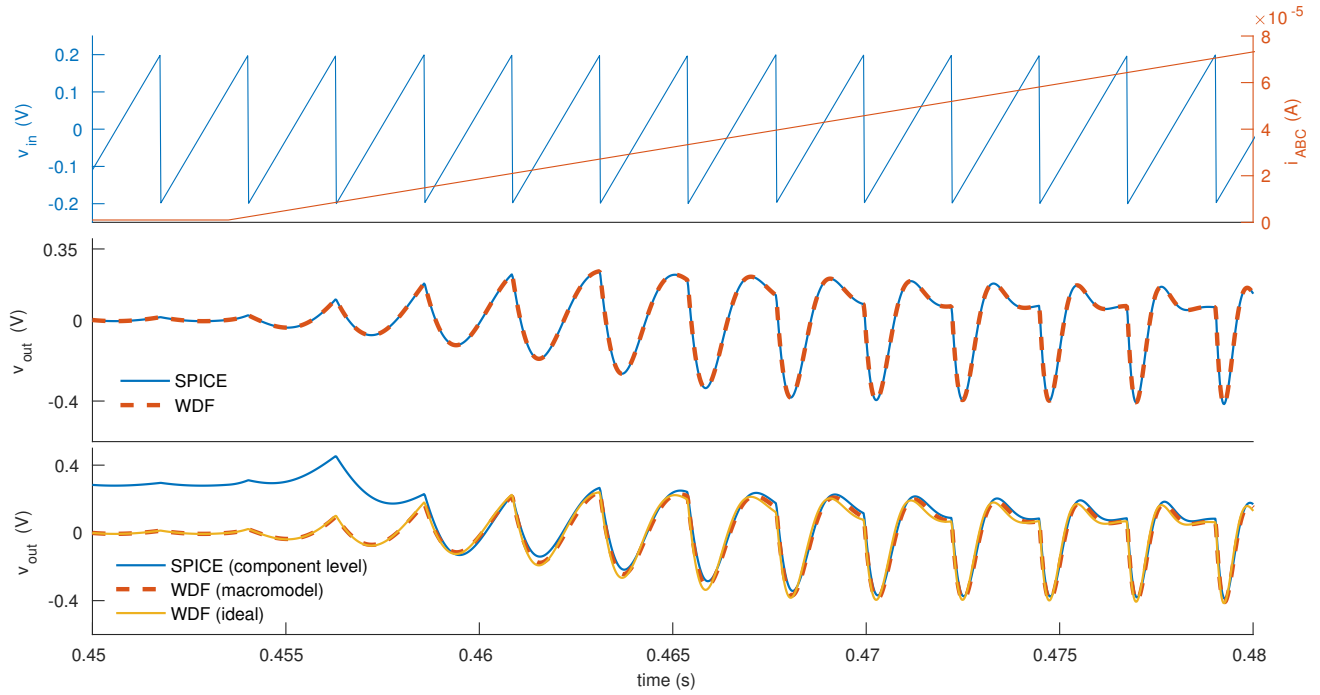

Figure 11: *Simulation of filter circuit under time-varying i_{ABC}.*

The clipping behavior of the OTA (3) will have a more pronounced effect as the amplitude of the input is increased. This will cause the differences between the simulations from the component-level SPICE model and the WDFs to deviate more at higher amplitudes than lower ones.

6. CONCLUSIONS

Two behavioral models of the operational transconductance amplifier, a commonly found component in audio circuits, were presented. How to incorporate the models into WDF was explained and a WDF model of an envelope filter was derived and simulated. Excellent results in the frequency domain were obtained when compared to an analytically derived transfer function of the filter section of the envelope filter while the results from a macromodel-based WDF performed well when compared to a component-level SPICE model of the LM13700 OTA.

The circuit was briefly studied under time-varying conditions and good results obtained when compared with state-of-the-art circuit simulation software, SPICE. In future work we hope to incorporate the clipping behavior of the OTA into our simulations. We hope also to further elaborate on the time-varying properties of WDFs in particular with respect to choice of s-to-z plane transform and/or numerical method as well as choice of wave variables.

7. REFERENCES

[1] R. Marston, "Understanding and using OTA op-amp ICs, part 1," *Nuts and Volts*, pp. 58–62, Apr. 2003.

[2] R. Marston, "Understanding and using OTA op-amp ICs, part 2," *Nuts and Volts*, pp. 70–74, May 2003.

[3] A. Gratz, "Operational transconductance amplifiers," Tech. Rep., 2008, Online: `synth.stromeko.net/diy/OTA.pdf`.

[4] T. Parveen, *Textbook of Operational Transconductance Amplifier and Analog Integrated Circuits*, I.K. International Pvt. Ltd., 2009.

[5] A. Huovilainen, "Enhanced digital models for analog modulation effects," in *Proc. Int. Conf. Digital Audio Effects (DAFx-05)*, Madrid, Spain, Sept. 2005.

[6] J. Pakarinen, V. Välimäki, F. Fontana, V. Lazzarini, and J. S. Abel, "Recent advances in real-time musical effects, synthesis, and virtual analog models," *EURASIP J. Adv. Signal Process.*, 2011.

[7] Roland Corporation, "Juno 60 service notes," Tech. Rep., Apr. 1983.

[8] Roland Corporation, "SH-101 service notes," Tech. Rep., Nov. 1982.

[9] Korg Electronic Laboratory Corporation, "MS-20 service notes," Tech. Rep., 1978.

[10] O. Kröning, K. Dempwolf, and U. Zölzer, "Analysis and simulation of an analog guitar compressor," in *Proc. Int. Conf. Digital Audio Effects (DAFx-11)*, Paris, France, Sept. 19–23, 2011.

[11] M. Holters and U. Zölzer, "Physical modelling of a wah-wah pedal as a case study for application of the nodal DK method to circuits with variable parts," in *Proc. Int. Conf.Digital Audio Effects (DAFx-11)*, Paris, France, Sept. 19–23, 2011.

[12] D. T. Yeh, J. S. Abel, and J. O. Smith, "Automated physical modeling of nonlinear audio circuits for real-time audio

effects—Part I: Theoretical development," *IEEE Trans. Audio, Speech, Language Process.*, vol. 18, no. 4, pp. 728–737, May 2010.

[13] A. Fettweis, "Wave digital filters: Theory and practice," in *Proc. IEEE*, 1986, vol. 74, pp. 270–327.

[14] S. Bilbao, *Wave and Scattering Methods for Numerical Simulation*, John Wiley & Sons, Ltd., 2005.

[15] A. Sarti and G. De Poli, "Toward nonlinear wave digital filters," *IEEE Trans. Signal Process.*, vol. 47, no. 6, pp. 1654–1668, 1999.

[16] S. Petrausch and R. Rabenstein, "Wave digital filters with multiple nonlinearities," in *Proc. 12th European Signal Process. Conf. (EUSIPCO)*, Sept. 2004, pp. 77–80.

[17] G. De Sanctis and A. Sarti, "Virtual analog modeling in the wave-digital domain," *IEEE Trans. Audio, Speech, Language Process.*, vol. 18, no. 4, pp. 715–727, 2010.

[18] J. Pakarinen and M. Karjalainen, "Enhanced wave digital triode model for real-time tube amplifier emulation," *IEEE Trans. Audio, Speech, Language Process.*, vol. 18, no. 4, pp. 738–746, May 2010.

[19] A. Bernardini and A. Sarti, "Dynamic adaptation of instantaneous nonlinear bipoles in wave digital networks," in *Proc. 24th European Signal Process. Conf. (EUSIPCO)*, Aug. 2016, pp. 1038–1042.

[20] M. Karjalainen and J. Pakarinen, "Wave digital simulation of a vacuum-tube amplifier," in *IEEE Int. Conf. Acoust., Speech, Signal Process.*, May 2006.

[21] S. D'Angelo, J. Pakarinen, and V. Välimäki, "New family of wave-digital triode models," *IEEE Trans. Audio, Speech, Language Process.*, vol. 21, no. 2, pp. 313–321, 2013.

[22] K. J. Werner, J. O. Smith III, and J. Abel, "Wave digital filter adaptors for arbitrary topologies and multiport linear elements," in *Proc. Int. Conf. Digital Audio Effects (DAFx-15)*, Trondheim, Norway, Nov. 2015.

[23] K. J. Werner, V. Nangia, J. O. Smith III, and J. S. Abel, "Resolving wave digital filters with multiple/multiport nonlinearities," in *Proc. Int. Conf. Digital Audio Effects (DAFx-15)*, Trondheim, Norway, Nov. 2015.

[24] A. S. Sedra and K. C. Smith, *Microelectronic Circuits*, Oxford University Press, New York, sixth edition, 2015.

[25] K. J. Werner, W. R. Dunkel, M. Rest, M. J. Olsen, and J. O. Smith III, "Wave digital filter modeling of circuits with operational amplifiers," in *Proc. 24th European Signal Process. Conf. (EUSIPCO)*, Budapest, Hungary, Aug. 2016.

[26] C. Acar, F. Anday, and H. Kuntman, "On the realization of OTA-C filters," *Int. J. Circuit Theory Appl.*, vol. 21, pp. 331–341, 1993.

[27] H. Kuntman, "Simple and accurate nonlinear OTA macromodel for simulation of CMOS OTA-C active filters," *Int. J. Electron.*, vol. 77, no. 6, pp. 993–1006, 1994.

[28] Texas Instruments, "LM13700 datasheet," Tech. Rep., Nov. 1999.

[29] R. L. Geiger and E. Sánchez-Sinencio, "Active filter design using operational transconductance amplifiers: A tutorial," *IEEE Circuits Devices Mag.*, vol. 1, no. 2, pp. 20–32, Mar. 1985.

[30] K. Meerkötter and T. Felderhoff, "Simulation of nonlinear transmission lines by wave digital filter principles," in *Proc. IEEE Int. Symp. Circuits Syst,*, May 1992, vol. 2, pp. 875–878.

[31] A. Bernardini, K. J. Werner, A Sarti, and J. O. Smith III, "Modeling nonlinear wave digital elements using the lambert function," *IEEE Transactions on Circuits and Systems I: Regular Papers*, vol. 63, no. 8, pp. 1231–1242, 2016.

[32] T. Schwerdtfeger and A. Kummert, "A multidimensional approach to wave digital filters with multiple nonlinearities," in *Proc. 22nd European Signal Process. Conf. (EUSIPCO)*, Lisbon, Portugal, Sept. 2014, pp. 2405–2409.

[33] C. Ho, A. Ruehli, and P. Brennan, "The modified nodal approach to network analysis," *IEEE Trans. Circuits Syst.*, vol. 22, no. 6, pp. 504–509, June 1975.

[34] K. J. Werner, *Virtual Analog Modeling of Audio Circuitry Using Wave Digital Filters*, Ph.D. dissertation, Stanford University, 2016.

[35] A. Bernardini, K. J. Werner, A. Sarti, and J. O. Smith III, "Modeling a class of multi-port nonlinearities in wave digital structures," in *Proc. 23rd European Signal Process. Conf. (EUSIPCO)*, 2015.

[36] K. J. Werner, W. R. Dunkel, and F. G. Germain, "A computational model of the Hammond organ vibrato/chorus using wave digital filters," in *Proc. Int. Conf. Digital Audio Effects (DAFx-16)*, Brno, Czech Republic, Sept. 2016, pp. 271–278.

[37] A. Fettweis and K. Meerkötter, "On adaptors for wave digital filters," *IEEE Trans. Acoust., Speech, Signal Process.*, vol. 23, no. 6, pp. 516–525, Dec. 1975.

[38] G. O. Martens and K. Meerkötter, "On N-port adaptors for wave digital filters with application to a bridged-tee filter," in *Proc. IEEE Int. Symp. Circuits Syst. (ISCAS)*, Munich, Germany, Apr. 1976, pp. 514–517.

[39] D. Fränken, J. Ochs, and K. Ochs, "Generation of wave digital structures for networks containing multiport elements," *IEEE Trans. Circuits Syst. I: Reg. Papers*, vol. 52, no. 3, pp. 586–596, Mar. 2005.

[40] Ó. Bogason, "Modeling audio circuits containing typical nonlinear components with wave digital filters," M.S. thesis, McGill University, Montreal, Quebec, Canada, 2017.

[41] G. Martinelli, "On the nullor," *Proc. IEEE*, vol. 53, no. 3, pp. 332, Mar. 1965.

[42] B. R. Myers, "Nullor model of the transistor," *Proc. IEEE*, vol. 53, no. 7, pp. 758–759, July 1965.

[43] L. T. Bruton, *RC-Active Circuits*, Prentice-Hall Inc, Englewood Cliffs, New Jersey, 1980.

[44] S. D'Angelo and V. Välimäki, "Wave-digital polarity and current inverters and their application to virtual analog audio processing," in *IEEE Int. Conf. Acoust., Speech, Signal Process. (ICASSP)*, Mar. 2012, pp. 469–472.

[45] A. B. Yildiz, "Modified nodal analysis-based determination of transfer functions for multi-inputs multi-outputs linear circuits," *Automatika*, vol. 51, no. 4, pp. 353–360, 2010.

[46] U. Zölzer, *Digital Audio Signal Processing*, John Wiley & Sons, Ltd., 2 edition, 2008.